The invisibility cloak: Chitin binding protein of *Verticillium nonalfalfae* disguises fungus from plant chitinases

Helena Volk[1], Kristina Marton[1], Marko Flajšman[1], Sebastjan Radišek[2], Ingo Hein[3,4], Črtomir Podlipnik[5], Branka Javornik[1], Sabina Berne[1]

[1]Department of Agronomy, Biotechnical Faculty, University of Ljubljana, Jamnikarjeva 101, SI-1000 Ljubljana, Slovenia; [2]Slovenian Institute of Hop Research and Brewing, Cesta Žalskega tabora 2, SI-3310 Žalec, Slovenia; [3]The James Hutton Institute, Invergowrie, Dundee DD2 5DA, Scotland, United Kingdom; [4]The University of Dundee, School of Life Sciences, Division of Plant Sciences at the JHI, Invergowrie, Dundee DD2 5DA, Scotland, United Kingdom; [5]Department of Chemistry and Biochemistry, Faculty of Chemistry and Chemical Technology, University of Ljubljana, Večna pot 113, SI-1000 Ljubljana, Slovenia

Corresponding author: S. Berne; E-mail: sabina.berne@bf.uni-lj.si

Nucleotide sequence data is available under accession numbers MH325205 for *VnaChtBP*, and MH325206 for *VaChtBP*.

Abstract

During fungal infections, plant cells secrete chitinases that digest chitin in the fungal cell walls. The recognition of released chitin oligomers via lysin motif (LysM)-containing immune receptors results in the activation of defence signalling pathways. We report here that *Verticillium nonalfalfae*, a hemibiotrophic xylem-invading fungus, prevents this recognition process by secreting a CBM18 (carbohydrate binding motif 18)-chitin binding protein, VnaChtBP, which is transcriptionally activated specifically during the parasitic life stages. VnaChtBP is encoded by the *Vna8.213* gene which is highly conserved within the species, suggesting high evolutionary stability and importance for the fungal lifestyle. In a pathogenicity assay, however, *Vna8.213* knockout mutants exhibit wilting symptoms similar to the wild type fungus, suggesting that *Vna8.213* activity is functionally redundant during fungal infection of hop. In binding assay, recombinant VnaChtBP binds chitin and chitin oligomers *in vitro* with submicromolar affinity and protects fungal hyphae from degradation by plant chitinases. Using a yeast-two-hybrid assay, homology modelling and molecular docking, we demonstrated that VnaChtBP forms dimers in the absence of ligands and that this interaction is stabilized by the binding of chitin hexamers with a similar preference in the two binding sites. Our data suggest that, in addition to chitin binding LysM (CBM50) and Avr4 (CBM14) fungal effectors, structurally unrelated CBM18 effectors have convergently evolved to prevent hydrolysis of the fungal cell wall against plant chitinases.

Introductory statements

Plant defense against pathogenic organisms relies on innate immunity, which is triggered by recognition of pathogen-derived or endogenous danger signals by plant receptors, described as pattern-triggered immunity (PTI) and effector-triggered immunity (ETI) (Jones and Dangl 2006; Dodds and Rathjen 2010). PTI, as a first line of defense, is activated by host cell surface-localized pattern recognition receptors (PRRs) sensing pathogen- and danger-associated molecular patterns (PAMPs and DAMPs, respectively) (Boller and Felix 2009; Böhm et al. 2014), which can be suppressed by pathogen virulence effectors (Dou and Zhou 2012). Host recognition of pathogen effectors by cytoplasmic nucleotide-binding domain leucine-rich repeat receptors (NLRs) leads to a second line of defense, ETI (Jones and Dangl 2006; Spoel and Dong 2012).

Pattern recognition receptors, which are either receptor-like kinases (RLKs) or receptor-like proteins (RLPs) that function in conjunction with RLKs, sense PAMPs or DAMPs and transduce downstream signaling to trigger PTI responses. Early PTI responses include the rapid generation of reactive oxygen species, activation of ion channels and mitogen-activated protein kinases. In turn, this leads to the expression of defense related genes, leading to an accumulation of antimicrobial compounds such as enzymes, which damage pathogen structures, inhibitors of pathogen enzymes and other antimicrobial molecules (Boller and Felix 2009; Dodds and Rathjen 2010; Macho and Zipfel 2014).

PAMPs, released during infection, are conserved molecular patterns characteristic of different pathogen classes (Ranf 2017). In fungi, chitin, in addition to beta-glucan and xylanase, is a well-studied PAMP that activates the host defense response. Chitin (a polymer of β-1,4-linked N-acetylglucosamine; $(GlcNAc)_n$), is a major and highly conserved component of fungal cell walls and can be degraded to chitin oligosaccharides by plant apoplastic chitinases. The generated chitin fragments are recognized by a chitin perception system and subsequently activate PTI (Shibuya and Minami 2001; Sanchez-Vallet et al. 2014; Shinya et al. 2015).

Major chitin sensing PRRs, RLKs and RLPs belonging to the LysM domain family, are well studied in *Arabidopsis* and rice (Gust et al. 2012; Ranf 2017). *Arabidopsis* LysM-RLK AtCERK1 (chitin elicitor receptor kinase1) binds N-acetylated chitin fragments with three LysM motifs and, through homodimer formation, mediates chitin-inducible plant defenses (Miya et al. 2007; Liu et al. 2012). Cao et al. (2014) later identified another LysM-RLK in *Arabidopsis*, AtLYK5, which binds chitin at higher affinity than AtCERK1. The authors propose that AtLYK5 functions as the major chitin receptor, which recruits AtCERK1 to form a chitin inducible receptor complex. In rice, two receptors are involved in chitin triggered immunity. LysM-RLP OsCEBiP (chitin elicitor binding protein) binds N-acetylated chitin fragments, which initiates receptor homodimerization and further heterodimerization with OsCERK1. This heterotetramer formation triggers chitin induced PTI (Hayafune et al. 2014).

To overcome chitin-triggered immunity, successful pathogens have evolved various strategies, including alteration of the composition and structure of cell walls, modification of carbohydrate chains and secretion of effector proteins to prevent hydrolysis of the fungal cell wall or the release and recognition of chitin oligosaccharides (Sanchez-Vallet et al. 2014).

A well-described strategy of fungal cell wall protection against host chitinases is that of the tomato leaf mold fungus *Cladosporium fulvum,* which secretes chitin-binding protein Avr4 during infection. Avr4 effector binds with its carbohydrate-binding module family 14 (CBM14) to the fungal cell wall chitin and thus shields fungal hyphae against degradation by chitinases (van den Burg et al. 2006; van Esse et al. 2007). There is evidence for a similar protection of cell wall chitin in a phylogenetically closely related species of the Dothideomycete fungi class harboring homologs of Avr4 (Stergiopoulos et al. 2010). Protection of fungal hyphae against hydrolysis by chitinases has also been shown for Mg1LysM and Mg3LysM of *Zymoseptoria tritici* (formerly *M. graminicola*) (Marshall et al. 2011). Furthermore, Vd2LysM from *Verticillium dahliae* (Kombrink et al. 2017) belongs to LysM fungal effectors which are known to bind chitin oligomers. The first LysM effector, Ecp6, was found in the tomato pathogen *C. fulvum* and its characterization provided evidence that Ecp6 specifically and with high affinity binds chitin oligosaccharides. This competition with receptors subsequently disrupts chitin recognition by host receptors and suppresses the chitin-triggered immune response (Bolton et al. 2008; de Jonge et al. 2010; Sánchez-Vallet et al. 2013). Genomes contain several genes for LysM effectors and those highly expressed during infection have been characterized in fungal pathogens, including *Z. tritici* (Marshall et al. 2011), *Magnaporthe oryzae* (Mentlak et al. 2012), *Colletotrichum higginsianum* (Takahara et al. 2016) and *V. dahliae* (Kombrink et al. 2017). These studies demonstrate the involvement of LysM effectors in pathogen virulence by scavenging chitin oligomers to prevent recognition by the host chitin receptors, thus suppressing the chitin-triggered immunity.

The question arises if there are other molecules/systems/complexes apart from Avr4 (CBM14) and LysM (CBM50) effectors that can interfere with plant chitin perception and activation of PTI. We have been studying the *Verticillium nonalfalfae* – hop (*Humulus lupulus* L.) pathosystem. In an early comparative transcriptomic study of compatible and incompatible interactions (Cregeen et al. 2015), an *in planta* expressed *V. nonalfalfae* lectin gene was detected. A preliminary study showed that this *V. nonalfalfae* lectin contains putative carbohydrate-binding module family 18, CBM18 (Wright et al. 1991) domains. CBM18 is a chitin-binding domain involved in recognition of chitin oligomers and typically found in fungal and plant proteins in one or more copies (Lerner and Raikhel 1992). We report here on the characterization of *V. nonalfalfae* lectin with six CBM18 domains and show that it is a novel effector in plant fungal pathogens. CBM18 binds chitin and protects hyphae of *Trichoderma viride* from hop chitinases in an *in vitro* protection assay.

Results

The majority of CBM18 module containing proteins of *V. nonalfalfae* are expressed *in planta*

The *Vna8.213* gene, encoding a putative pathogen CBM18-containing chitin binding protein (VnaChtBP), has previously been identified as a differentially expressed transcript during compatible and incompatible interactions of *V. nonalfalfae* and hop (Cregeen et al. 2015). Surveying the *V. nonalfalfae* genome (Jakše et al. 2018) uncovered ten additional genes that encode for proteins with at least one CBM18 module (Fig. 1). These genes were grouped into four categories according to their domain architecture: Lectin-like proteins (Fig. 1 A), Chitinases (Fig. 1 B), Chitin deacetlyases (Fig. 1 C) and Xyloglucan endotransglucosylase (Fig. 1 D). The size of these proteins ranged between 349 and 1,696 amino acids (Vna6.1 and Vna1.668, respectively) and they harbored between one to ten CBM18 modules. Amongst these genes, ten are differentially expressed *in planta* (Fig. 1 E) (Marton et al. 2018) and five (Vna2.980, Vna6.6, Vna8.213, Vna9.506 and Vna9.510) were predicted to be classically secreted proteins with N-terminal signal peptides. Amongst the chitinases (Fig. 1 B), transcripts of *Vna3.655* and *Vna9.506* were detected exclusively in susceptible hop, *Vna1.668* transcripts were found expressed in the roots of both resistant ('Wye Target') and susceptible ('Celeia') hop varieties, while transcripts of *Vna2.980* and *Vna9.510* were barely detectable. Interestingly, only one chitin deacetylase gene (*VnaUn.355*) was expressed during infection, and it showed preferential induction in the roots of both hop varieties. Such an expression profile was also evident for transcripts of *Vna6.6* belonging to xyloglucan endotransglucosylase. The highest expression was observed for *Vna8.213* transcripts, in particular at the late stages of infection of susceptible hop. Interestingly, *Vna1.667* gene-encoding lectin-like protein, containing 10 CBM18 modules, was barely expressed in the roots of susceptible hop during the early infection stages.

To confirm the expression patterns of *Vna8.213* measured by RNA-Seq, detailed gene expression profiling of root and shoot samples from susceptible and resistant hop varieties was performed using RT-qPCR at 6, 12 and 18 days post-inoculation (dpi) with *V. nonalfalfae* (Fig. 2). Gene expression of *Vna8.213*, from here on designated as *VnaChtBP*, increased with time, reaching the highest abundance in stems of susceptible hop at 18 dpi. The overall *VnaChtBP* expression in resistant hop was at a much lower level than in the susceptible variety and peaked at 12 dpi in stems. These results indicate that *VnaChtBP* expression is induced *in planta* and its transcript abundance in susceptible hop increases with progression of fungal colonization.

Sequence conservation suggests evolutionary stability of *VnaChtBP*

To investigate the presence and sequence variation of *VnaChtBP* in 28 *V. nonalfalfae* isolates (Suppl. Table S1), PCR amplification and Sanger sequencing of cloned genes was performed. The *VnaChtBP* gene was present in all analyzed isolates and displayed no sequence polymorphisms. This is consistent with purifying selection and suggests evolutionary stability of the gene as well as an important role in the fungal lifestyle.

Among all sequences deposited at NCBI, VnaChtBP shared the highest protein identity with a lectin from *V. alfalfae* (97%; an alfalfa isolate VaMs.102), followed by *V. dahliae* lectin-B (80%; a lettuce isolate VdLs.17), two *V. dahliae* hypothetical proteins, Vd0004_g7043 and Vd0001_g7025 (80% and 79%; strawberry isolates 12161 and 12158), and a hypothetical protein BN1708_012400 from *V. longisporum* (78%; a rapeseed isolate VL1) (Suppl. Table S2). Additional homologs (Suppl. File S1), but with lower identity (48-39%), were identified in fungi amongst Sordariomyceta (40) and Dotideomyceta (3), and in fungi *Incertae sedis* amongst Neocallimastigomycetes (5) and Chytridiomycetes (2).

Due to the high sequence similarity shared between VnaChtBP and *V. alfalfae* VaMs.102 lectin, PCR screening and Sanger sequencing of amplicons from four additional *V. alfalfae* isolates was carried out. As with *VnaChtBP*, no allelic polymorphisms were found among the sequences obtained and comparison of *V. nonalfalfae* and *V. alfalfae* gene sequences from these isolates also showed 97% sequence identity. Within the 36 single nucleotide polymorphisms identified, only resulted in 13 amino acid substitutions (Suppl. File S2).

VnaChtBP forms dimers and has two potential binding sites for interaction with chitin

V. nonalfalfae VnaChtBP is an intronless gene and predicted to encode for a cysteine rich (12.5%) apoplastic effector (VnaChtBP) with 400 amino acids, including N-terminal signal peptide and six type 1 Chitin binding domains (ChtBD1; PF00187). This domain is classified in the CAZY database (Lombard et al. 2014) as Carbohydrate-binding module 18 (CBM18) and consists of 30 to 43 residues rich in glycines and cysteines, which are organized in a conserved four-disulfide core (Wright et al. 1991; Andersen et al. 1993; Asensio et al. 2000). It is a common structural motif, with a consensus sequence X3CGX7CX4CCSX2GXCGX5CX3CX3CX2 (Prosite PS50941), found in various plant and fungal defense proteins and is involved in the recognition and/or binding of chitin subunits (Finn et al. 2014).

Since many chitin binding proteins have been reported to form dimers (Liu et al. 2012; Sánchez-Vallet et al. 2013; Cao et al. 2014), a yeast-two-hybrid assay was carried out using *VnaChtBP* both as bait and prey to study the ability to dimerize. Dimer formation of VnaChtBP was detected on a minimal media using histidine as a reporter (Fig. 3 A). Consistent with a weak interaction, only limited growth was observed on triple dropout reporter media (synthetic complete medium without leucine, tryptophan and uracil) and the X-gal reporter was not activated.

To understand the chitin binding mechanism of CBM18 effectors better, homology modelling of VnaChtBP 3D structure was performed. The SWISS-MODEL server produced three models based on different templates, shown in Table 1. Model02 provided the best fit for four out of six CBM18 modules and was used as the basis of the characterization. Molecular docking of the chitin hexamer into the VnaChtBP model (Fig. 3 B) shows that each protein monomer contributes to the formation of two binding sites accessible to the ligand. In binding site I (BSI), chitin hexamer is accommodated in a shallow groove formed by four hevein domains of polypetide chain A and two hevein domains of chain B, while binding site II (BSII) is comprised of four hevein domains of chain B and two domains of chain A. According to the analysis of the presented complex with YASARA, the binding of chitin hexamer in the BSI is strengthened by eleven (four accepted and seven donated) hydrogen bonds and eight hydrophobic

interactions, which contribute to the total binding energy of 6.891 kcal/mol (AutoDock/Vina) and an estimated dissociation constant of 8.88 µM. Similar preference for binding of chitin hexamer in the BSII was observed, with an estimated dissociation constant of 2.01 µM and the total binding energy of 7.772 kcal/mol, supported by eight (three accepted, five donated) hydrogen bonds and 12 hydrophobic interactions between the ligand and receptor.

VnaChtBP binds chitin *in vitro* and protects fungal hyphae against plant chitinases

To confirm carbohydrate binding, *E. coli* produced and Ni-NTA affinity purified recombinant VnaChtBP (Suppl. Fig. S1) was used in a sedimentation assay with various carbohydrates. VnaChtBP binds specifically to chitin polymer, in the form of chitin beads and crab shell chitin, but not to the plant cell wall polymers cellulose and xylan (Fig. 4). To examine the affinity of VnaChtBP binding to chitin in more detail, recombinant protein was immobilized to the CM5 sensor chip and the VnaChtBP interaction with chitin hexamer was analyzed using surface plasmon resonance (SPR) (Kastritis and Bonvin 2013). VnaChtBP reveals concentration-dependent binding of chitin hexamer (Fig. 5) with a dissociation constant of 0.78 ± 0.58 µM, while no specific binding to other tested carbohydrates was detected (Suppl. Fig. S2). Since the chitin binding affinity of the protein increases for longer chitin oligomers (Asensio et al. 2000), this value is comparable to other reported chitin oligomer binding affinities of fungal effectors but exceeds by one order of magnitude those reported for *Arabidopsis* chitin recognition receptors and hevein (Table 2).

Chitin binding effectors have been reported to protect fungal hyphae from plant chitinases (van den Burg et al. 2004; Marshall et al. 2011). To determine whether recombinant VnaChtBP can protect fungal cell walls against hydrolysis by plant chitinases , a cell protection assay adapted from Mentlak et al. (2012) was performed using germinating conidia of *Trihoderma viride* and extracted xylem sap from *V. nonalfalfae* infected hop (Flajšman et al. 2017a) as a source of plant chitinases (containing 19 U of chitinase/mg total protein). In the presence of xylem sap, only minimal germination of the *T. viride* conidia occurred after 24 h incubation, while a pre-incubation in a 3 µM solution of recombinant VnaChtBP prior to the addition of xylem sap, enabled germination of conidia and hyphal growth. Interestingly, aggregation and compaction of fungal hyphae was detected only in the presence of both xylem sap and VnaChtBP, while normal mycelial growth without hyphal aggregation was observed in the solution of VnaChtBP (Fig. 6). We assume that VnaChtBP by binding and probably surrounding chitin fibers in the fungal cell wall, masks chitin and protects it from degradation by xylem sap chitinases.

VnaChtBP deletion has no significant effect on the growth and pathogenicity of *V. nonalfalfae*

Since *VnaChtBP* is specifically expressed during colonization of hop, its contribution to fungal virulence was tested in the susceptible hop variety 'Celeia'. *V. nonalfalfae* knockout mutants of *VnaChtBP* were generated by targeted gene disruption via *A. tumefaciens*-mediated transformation. Prior to plant inoculation, growth of fungal colonies and sporulation of knockout mutants were assessed *in vitro* and compared to wild type. In the selected knockout mutants, mycelial growth and fungal morphology did not differ significantly from the wild type. Reduced sporulation was observed for both mutants compared to the wild type but this did not impact on disease frequency (Suppl. Fig. S3). After inoculation

of hop plants, disease symptoms were independently assessed five times using a disease severity index (DSI) with a 0-5 scale (Radišek et al. 2003). After the final symptom assessment, the presence of fungus in all inoculated plants was confirmed through re-isolation tests and qPCR with fungus specific markers (Cregeen et al. 2015). Figure 7 shows symptom development in susceptible hop following infection with the wild type *V. nonalfalfae* and knockout mutants of *VnaChtBP*. Both *VnaChtBP* deletion mutants displayed Verticillium wilting symptoms (chlorosis and necrosis of the leaves) in susceptible hop similar to the wild type fungus, with no significant differences among them according to the DSI assessment. Independent pathogenicity assays with additional *VnaChtBP* deletion mutants yielded the same results (data not shown). This suggests that VnaCthBP function is redundant for *V. nonalfalfae* infection.

Discussion

V. nonalfalfae, a soil born fungal pathogen, causes serious economic damage in European hop growing regions. Significant efforts have been invested to study the molecular mechanisms of Verticillium wilt in hop and fungus pathogenicity (Radišek et al. 2006; Jakše et al. 2013; Cregeen et al. 2015; Mandelc and Javornik 2015; Flajšman et al. 2016; Jakše et al. 2018; Marton et al. 2018).

In planta expressed fungal proteins are potential effector candidates, which might be implicated in pathogen virulence. The here studied effector candidate *V. nonalfalfae VnaChtBP*, encodes for a CBM18 domain containing chitin binding protein and is highly expressed in hop plants. Using an established bioinformatic pipeline (Marton et al. 2018), we identified eleven genes in the *V. nonalfalfae* genome that contain CBM18 domains. Of these genes, two harboured a single CBM18 domain (Fig. 1) and five, including *VnaChtBP*, contain a predicted N-terminal signal peptide. Although CBMs play a key role in the recognition of carbohydrates and are known to promote efficient substrate hydrolysis as a part of carbohydrate-active enzymes (e.g., CBM18 motifs found in chitinases), they have also been found to be present in toxins, virulence factors or pathogenesis-associated proteins (Guillén et al. 2010). Proteins containing CBM18 motifs are common in fungi, particularly in plant and animal pathogens. Indeed, they are almost three times as common in the proteomes of pathogens than in those of non-pathogenic fungi across the phylum Ascomycota (Soanes et al. 2008). Intriguingly, in *Verticillium* spp., CBM18 containing genes are more frequently observed in saprophytic *V. tricorpus* (13) (Seidl et al. 2015) than in pathogenic *V. dahliae* and *V. alfalfae* (9). The expansion of CBM18 domains in ChtBPs, could be linked to the evolution of pathogenicity, and has, for example, been reported in the fungal pathogen *B. dendrobatidis*, which has caused a worldwide decline of the amphibian populations (Abramyan and Stajich 2012). In total, eighteen genes with between one to eleven CBM18 domains have been identified in *B. dendrobatidis* including some classified as lectin-like proteins. Biochemical characterization of three such lectin-like proteins revealed that two have a signal peptide and co-localize with chitinous cell wall in *Saccharomyces cerevisiae*. Furthermore, one of these proteins has been shown to bind chitin and thereby protect *Trichoderma reesei* from exogenous chitinase, suggesting a role of lectin-like proteins in fungal defence (Liu and Stajich 2015). Similarly, in the rice blast fungus *M. oryzae*, 15 genes with one to four CBM18 domains were found, although gene-targeted disruption and tolerance to chitinase treatment did not support the implication of the tested genes in fungal pathogenicity (Mochizuki et al. 2011).

VnaChtBP consists of six tandemly repeated CBM18 motifs, contains a signal peptide and is predicted to reside in the apoplasm, which is consistent with the role of chitin binding in the extracellular space. Homology search of proteins that contain CBM18 motifs in other *Verticillium* species, revealed that this type of protein is common in pathogenic *Verticillium* species but it seems not to be ubiquitous. For example, in the recently sequenced genomes of five *V. dahliae* strains isolated from strawberry, three strains harbored ChtBPs with five, six and ten CBM18 motifs, while none were detected in two other strains.

Monitoring the *in planta* expression of *VnaChtBP* showed that it is highly expressed at the later stages of infection in a susceptible hop cultivar, and continuous to be expressed even at 30 dpi, when plants exhibit severe wilting symptoms (Cregeen et al. 2015; Marton et al. 2018). In contrast, in a resistant cultivar, the *VnaChtBP* gene is slightly induced after infection and then completely down-regulated. The expression pattern of the *VnaChtBP* gene coincides with *V. nonalfalfae* colonization of hop, whereby the fungus spread is unimpeded in susceptible plants while colonization is arrested around 12-20 dpi in resistant hop plants, presumably due to strong plant resistance responses (Cregeen et al. 2015). The immune reaction in incompatible interaction is unlikely to impose selection pressure on the *VnaChtBP* gene since no allelic polymorphisms were detected among analysed *V. nonalfalfae* isolates. Similarly, no allelic variation was found in the closest (97% identity) homolog to the *VnaChtBP* gene from isolates of *V. alfalfae*, suggesting highly conserved genes. Allelic variation is commonly detected in fungal proteins that function as avirulent (Avr) determinants upon perception by the host defence, but not necessarily in virulence factors of the pathogen (Stergiopoulos et al. 2007). Taken together, we speculate that the absence of allelic variation and the high gene expression observed *in planta* suggest a role for VnaChtBP in virulence of *V. nonalfalfae*. However, in pathogenicity assay, *VnaChtBP* targeted deletion mutants were not significantly impaired in their hops infectivity compared to wild type fungus which is in line with functional redundancy. Unchanged virulence of deletion mutants, presumably due to functional redundancy, has been reported for two other tested CBM18-containing ChtBPs in *M. oryzae* (Mochizuki et al. 2011) and also for LysM fungal effector, Mg1LysM of *Mycosphaerella graminicola* (Marshall et al. 2011). Indeed, other putative ChtBPs have been found in the *V. nonalfalfae* genome, which may have a role in protection of the fungal cell wall chitin or may interfere with chitin-triggered plant immunity. Specifically, Vna9.508, with one LysM domain, and Vna8.102, with five LysM domains, are both expressed during infection of hop and predicted to be secreted proteins with apoplastic localization (Marton et al. 2018). Orthologues of *C. fulvum* Avr4 with CBM14 chitin-binding motif were not identified in the *V. nonalfalfae* genome (Jakše et al. 2018) or in the predicted proteomes of other *Verticillium* species (Seidl et al. 2015).

Consistent with previously characterized CBM18 containing proteins from *M. oryzae* (Mochizuki et al. 2011) and *B. dendrobatidis* (Liu and Stajich 2015), recombinant VnaChtBP binds specifically to chitin beads and crab shell chitin, but not to plant cell wall cellulose or xylan. In addition to chitin polymer, recombinant VnaChtBP also binds chitin hexamer in an SPR experiment, with binding affinity in the submicromolar range. Compared to plant chitin receptors, recombinant VnaChtBP alongside LysM effectors Ecp6 from *C. fulvum*, Slp1 from *M. oryzae* (Mentlak et al. 2012), ChELP1 and ChELP2 from *C. higginsianum* (Takahara et al. 2016) exhibit three to five orders of magnitude higher affinity to chitin

298 oligomers. It is thus not surprising that these fungal effectors are able to outcompete plant chitin
299 receptors, such as *Arabidopsis thaliana* AtLYK5 (Cao et al. 2014) and AtCERK1 (Liu et al. 2012).

300 Based on NMR studies and solved crystal structures of plant LysM chitin receptors, several mechanisms
301 for binding of chitin have been proposed; from a simple 'continuous groove' model for AtCERK1 (Liu et
302 al. 2012) to the OsCEBiP 'sandwich' (Hayafune et al. 2014) and 'sliding mode' model (Liu et al. 2016).
303 However, these models have been unable to explain the observed elicitor activities of chitin oligomers.
304 Building on these models and using a range of chitosan polymers and oligomers bound to *Atcerk1*
305 mutants resulted in an improved 'slipped sandwich' model that fits all experimental results (Gubaeva et
306 al. 2018). A recent structural study of fungal LysM effector Ecp6 from *C. fulvum* revealed a novel chitin
307 binding mechanism that explained how LysM effectors can outcompete plant host receptors for chitin
308 binding (Sánchez-Vallet et al. 2013). Ecp6 consists of three tightly packed LysM domains, with a
309 typical βααβ fold. Intra-chain dimerization of chitin-binding regions of LysM1 and LysM3 leads to the
310 formation of a deeply buried chitin binding groove with an ultra-high (pM) affinity. The remaining LysM2
311 domain also binds chitin, albeit with low micromolar affinity, and interferes with chitin-triggered
312 immunity, possibly by preventing chitin immune receptor dimerization and not by chitin fragment
313 sequestering, as in case of LysM1-LysM3.

314 To date, to the best of our knowledge, the molecular mechanism of chitin binding of CBM18 fungal
315 effectors remains elusive. However, the 3D homology model of VnaChtBP provides a tangible model for
316 the molecular docking of the chitin hexamer. Although only four out of six CBM18 domains could be
317 reliably modelled, the analysis revealed that VnaChtBP dimerizes. Importantly, this prediction was
318 independently validated through a yeast-two-hybrid experiment. The VnaChtBP complex has two
319 putative chitin binding sites which form a shallow binding cleft by cooperation of both polypeptide
320 chains and have a similar preference to chitin. As in CBM18 lectin-like plant defence proteins (Jiménez-
321 Barbero et al. 2006), typically represented by a small antifungal protein hevein from the rubber tree
322 (*Hevea brasiliensis*), a network of hydrogen bonds and several hydrophobic interactions occur between
323 VnaChtBP residues and N-acetyl moieties of the chitin oligomer. These are thought to stabilize the
324 interaction and contribute to submicromolar chitin binding affinity, as determined by SPR. Similarly, the
325 recently solved crystal structure of fungal effector CfAvr4, a CBM14 lectin, in complex with chitin
326 hexamer (Hurlburt et al. 2018) has revealed that two effector molecules form a sandwich structure,
327 which encloses two parallel stacked chitin hexamer molecules, shifted by one sugar ring, in an extended
328 chitin binding site. In this complex, the interaction is mediated through aromatic residues and numerous
329 hydrogen bonds with both side chains and main chains. Interestingly, no intermolecular protein-protein
330 interactions have been observed across the dimer, suggesting ligand induced effector dimerization. Site-
331 directed mutagenesis of residues responsible for binding of chitin hexamer showed that ligand binding
332 function is independent from recognition by host resistance protein Cf-4.

333 Fungal plant pathogens have evolved several strategies to escape the surveillance of chitin-related
334 immune systems (Sanchez-Vallet et al. 2014). The different mechanisms used include conversion of
335 chitin to chitosan by chitin deacetylases and inclusion of α-1,3-glucan in the cell walls, as well as
336 secretion of diverse effectors that can shield the fungal hyphae from hydrolysis by plant chitinases,
337 directly inhibiting their activity, acting as scavengers of chitin fragments or preventing chitin–induced

receptor dimerization. Secreted effector Avr4 from *C. fulvum* binds to fungal cell wall chitin to reduce its accessibility to host chitinases (van den Burg et al. 2006). Similar to CfAvr4, wheat pathogen *M. graminicola* secreted effectors Mg1LysM and Mg3LysM protect fungal hyphae from hydrolysis by plant chitinases (Marshall et al. 2011). We provide evidence that, in addition to Avr4 (CBM14) and LysM (CBM50) effectors, structurally unrelated CBM18 lectin-like proteins that are found in fungal pathogens of plants (this study) and amphibian pathogens (Liu and Stajich 2015) have evolved a chitin shielding ability against plant chitinases.

Materials and Methods

Maintenance of plant cultures and cultivation of microorganisms

Nicotiana benthamiana seedlings were grown at 23 ± 2°C under a 16:8 photoperiod. Hop (*Humulus lupulus* L.) of susceptible 'Celeia' and resistant 'Wye Target' cultivars were grown as described previously (Flajšman et al. 2017b). *Escherichia coli* MAX Efficiency DH5α or MAX Efficiency DH10B (both from Invitrogen, ThermoFisher Scientific) were used for plasmid propagation and were grown at 37°C on LB agar plates or liquid medium supplemented with appropriate antibiotics (carbenicillin 100 mg/liter, kanamycin 50 mg/liter, spectinomycin 100 mg/liter or gentamicin 25 mg/liter). *E. coli* Shuffle T7 (New England Bioloabs) were propagated at 30°C and protein expression was performed at 16°C. *Trichoderma viride* was obtained from The Microbial Culture Collection Ex (IC Mycosmo (MRIC UL)) and all *Verticillium* strains were from the Slovenian Institute of Hop Research and Brewing fungal collection. Fungi were grown at 24°C in the dark on ½ Czapek-Dox agar plates or liquid medium. Knockout mutants were retrieved from selection medium supplemented with 150 mg/liter timentin and 75 mg/liter hygromycin. For agroinfiltration, *Agrobacterium tumefaciens* MV3101 was grown at 28°C on YEB agar plates or liquid medium supplemented with rifampicin 25 mg/liter, gentamicin 25 mg/liter, and spectinomycin 50 mg/liter.

RNA sequencing

RNA-Seq library preparation from *V. nonalfalfae* infected hop at 6, 12, 18 and 30 days post inoculation (dpi) and data processing have been previously described (Progar et al. 2017). Fungal transcripts were filtered out and their gene expression profiles were generated using the Hierarchical clustering with Euclidean distance method in R language (R Core Team 2016). Data were presented as a matrix of $\log_2$CPM (counts per million–number of reads mapped to a gene model per million reads mapped to the library) expression values.

VnaChtBP gene expression profiling with RT-qPCR

The expression of *VnaChtBP* was quantified by RT-qPCR in hop infected with *V. nonalfalfae* isolate T2. Total RNA was extracted at 6, 12, and 18 dpi using a Spectrum Plant total RNA kit (Sigma-Aldrich) and 1 µg was reverse transcribed to cDNA using a High Capacity cDNA reverse transcription kit (Applied Biosystems). The qPCR reaction was run in 5 biological and 2 technical replicates on an ABI PRISM 7500

(Applied Biosystems), under the following conditions: denaturation at 95°C for 10 min, followed by 40 cycles at 95°C for 10 s, 60°C for 30 s, and consisted of: 50 ng of cDNA, 300 nM forward and reverse primer, and 5 µl of Fast SYBR Green master mix (Roche). The results were analyzed using the $\Delta\Delta C_t$ method (Schmittgen and Livak 2008). Transcription levels of *VnaChtBP* were quantified relative to its expression in liquid Czapek-Dox medium and normalized to fungal biomass in hop using topoisomerase and splicing factor as reference genes (Marton et al. 2018). Primers used are listed in Table 3.

Genetic analysis

Genomic DNA was extracted from 7-10 day PDA cultured *Verticillium* isolates by the CTAB extraction method (Möller et al. 1992). PCR reactions were performed in 50 µl using Q5® High-Fidelity DNA Polymerase (NEB), 500 nM gene-specific primers (Table 3) and 100 ng DNA under the following conditions: denaturation at 95°C for 10 min, followed by 40 cycles at 95°C for 10 s, 58°C for 30 s, 72°C for 90 s, and a final elongation step at 72°C for 90 s. PCR products were purified from agarose gel (Silica Bead DNA Gel Extraction Kit, Fermentas), cloned into pGEM®-T Easy vector (Promega) and sequenced using Sanger technology with gene-specific and plasmid-specific primers (Table 3). Sequences were analyzed using CodonCode Aligner V7.1.2 (CodonCode Co.) and deposited at the NCBI.

Bioinformatic analysis

A putative localization of VnaChtBP to the apoplast was predicted with ApoplastP 1.0 (Sperschneider et al. 2017). To classify *V. nonalfalfae* CBM18-containing proteins functionally, sequence based searches were carried out using the FunFHMMer web server at the CATH-Gene3D database (Dawson et al. 2017). To obtain VnaChtBP homologs, the amino acid sequence of VnaChtBP was used as a query for NCBI BLAST+ against UniProt Knowledgebase at Interpro (Li et al. 2015).

Yeast-two-hybrid assay

Dimerization of VnaChtBP was examined with a yeast-two-hybrid experiment using the ProQuest Y2H system (Invitrogen). To generate bait and prey vectors, the *VnaChtBP* gene was cloned into pDEST22 and pDEST32, respectively, and co-transformed in yeast. The interactors were confirmed by plating the yeast co-transformants on triple dropout reporter medium SC-LWH (synthetic complete medium without leucine, tryptophan and histidine), on triple dropout reporter medium SC-LWU (synthetic complete medium without leucine, tryptophan and uracil) and by performing an X-gal assay. The self-activation test of a pDEST22 construct containing *VnaChtBP* gene with empty pDEST32 vectors was also performed.

3D modelling and molecular docking

The SWISS-MODEL (Arnold et al. 2006; Waterhouse et al. 2018) server produced three models based on different templates and Model02 was selected for further modelling. The output protein structure was additionally minimized in explicit water using an AMBER14 force field (Duan et al. 2003) and 'em_runclean.mcr' script within YASARA Structure (Krieger and Vriend 2014, 2015). A 3D structure model of chitin hexamer was built with SWEET PROGRAM v.2 (Bohne et al. 1998, 1999), saved as a PDB file and used as a ligand in subsequent molecular docking experiments with AUTODOCK/VINA (Trott and Olson 2009), which is incorporated in YASARA Structure. To ensure the integrity of docking results, 200 independent dockings of the ligand to the receptor were performed. The pose with the best docking

score was selected for further refinement using 'md_refine.mcr' script provided by YASARA Structure. The final model of the hexameric chitin bound to the VnaChtBP dimer was then used for the analysis.

Recombinant protein production

VnaChtBP DNA without predicted signal peptide (SignalP 4.1) was cloned into a pET32a expression vector using a Gibson Assembly® Cloning Kit (NEB). The protein expression in *E. coli* SHuffle® T7 cells (NEB) was induced at OD_{600} = 0.6 with 1 mM IPTG and incubated overnight at 16°C. The recombinant protein was solubilized from inclusion bodies using a mild solubilization method (Qi et al. 2015). Briefly, pelleted cells were resuspended in cold PBS buffer and disrupted by sonication. After centrifugation, the pellet was washed with PBS, resuspended in urea, frozen at -20°C and slowly allowed to thaw at RT. The recombinant protein was purified using Ni-NTA Spin Columns (Qiagen) according to the manufacturer's protocol, aliquoted and stored in 20 mM Tris (pH 8.0) at -80°C.

Carbohydrate sedimentation assay and Western blot detection

The carbohydrate sedimentation assay was adapted from (van den Burg et al. 2006). Briefly, 15 µg of recombinant VnaChtBP in 20 mM Tris (pH 8.0) was mixed with 1.5 mg of chitin magnetic beads (NEB), crab shell chitin (Sigma-Aldrich), cellulose (Sigma-Aldrich) or xylan (Apollo Scientific) and incubated at RT for 2 h on an orbital shaker at 350 rpm. The same amount of protein in Tris buffer without added carbohydrates was used as a negative control. After centrifugation (5 min, 13,000 g), the supernatant was collected and the pellet was washed three times with 800 µl 20 mM Tris (pH 8.0) prior to resuspension in 4X Bolt™ LDS Sample Buffer with the addition of reducing agent (Invitrogen).

The presence of VnaChtBP in different fractions was determined by WB analysis. Samples (25 µL) were loaded on a precast Bolt™ 4-12% Bis-Tris gel (Invitrogen) and SDS-PAGE in 1x MOPS running buffer was performed using a Mini Gel Tank (ThermoFisher Scientific) for 30 min at 200 V. Proteins were transferred for 1 h at 30 V to an Invitrolon PVDF membrane (Invitrogen) and Ponceau S stained. The membrane was blocked with 5% BSA in 1x PBS before the addition of the primary antibody His-probe (H-3) (SCBT) (1:1,000). The membrane was incubated overnight at 4°C, washed with 1x PBS and incubated in a solution of secondary Chicken anti-mouse IgG-HRP (SCBT) (1:5,000) for 1 h. Protein bands were detected using Super Signal West Pico (ThermoFisher Scientific) ECL substrate in a GelDoc-It2 Imager (UVP).

Surface plasmon resonance

The binding of hexa-N-acetyl chitohexaose ($(GlcNAc)_6$; IsoSep) to VnaChtBP was measured using a Biacore T100 analytical system and CM5 sensor chip (Biacore, GE Healthcare). The CM5 sensor chip was activated using an Amine coupling Kit (GE Healthcare) according to the manufacturer's instructions. VnaChtBP was diluted into 10 mM Sodium acetate pH 5.1 to a final concentration of 0.1 mg/ml and injected for five minutes over the second flow cell. The first flow cell was empty and served as a reference cell to control the level of non-specific binding. The final immobilization level was approximately 10,000 response units (RU). The $(GlcNAc)_6$ stock solution was diluted into a series of concentrations (0.05, 0.1, 0.2, 0.4, 0.8, 1.6, 3.2 and 6.4 µM) with the HBS buffer (10 mM HEPES, 140 mM NaCl, pH 7.4) and assayed to detect direct binding to VnaChtBP. Titration was performed in triplicate. In addition to chitin hexamer, N-acetyl glucosamine, glucosamine, glucose, galactose and mannose were tested at a 500 µM concentration in HBS buffer. Biacore T100 Evaluation software was used to assess the

results. First, the sensorgrams were reference and blank subtracted, then a Steady State Affinity model was applied to calculate the affinity constant (K_d). The average of three repeated experiments was used for final K_d determination.

Xylem sap extraction and chitinase activity assay

Xylem sap was extracted from infected hop plants in a pressure chamber at 0.2 MPa for 120 min (Flajšman et al. 2017a). Chitinase activity of xylem sap was determined by mixing 150 µl of xylem sap, or 100 mM Na-acetate (pH 5.0) buffer as negative control, with 1.5 mg of Chitin Azure (Sigma-Aldrich) dissolved in 150 µl 100 mM Na-acetate (pH 5.0). The samples were incubated for 150 min at 25°C on a rotatory shaker at 70 rpm. An aliquot of 80 µl was taken immediately (blank sample) and after 150 min. The reaction was stopped with the addition of 20%v/v HCl and samples were centrifuged for 10 min at 10,000 g. The chitinase activity of xylem sap in the supernatant was determined by measuring the absorbance of released Remazol Brilliant Blue dye at 575 nm against 100 mM Na-acetate (pH 5.0). One enzyme unit was defined as the amount of chitinase that produced a 0.01 increase in absorbance at 575 nm, measured at 25°C and pH 5.0. The total protein concentration of the xylem sap was measured in a 10x diluted sample using a Pierce™ BCA Protein Assay Kit (Thermo Scientific) following the standard protocol.

Cell Protection Assay

The cell protection assay was adapted from Mentlak et al., 2012. *Trihoderma viride* conidia were harvested, diluted to 2,000 conidia/ml in 50 µl ½ Czapek-dox medium and incubated overnight. After germination of the conidia, 25 µl of recombinant VnaChtBP (3 µM final concentration) or an equal volume of storage buffer (20 mM Tris; pH 8.0) were added and the conidial suspensions were incubated for 2 h. Fungal cell wall hydrolysis was triggered by the addition of 25 µl of xylem sap as a source of plant chitinases, while 25 µl of Na-acetate (100 mM; pH 5.0) was used in the control experiment. After 24 h incubation, mycelia formation and fungal growth were examined using a Nikon Eclipse 600 microscope.

Pathogenicity assay

VnaChtBP knockout mutants were generated using the *Agrobacterium tumefaciens* mediated transformation protocol described previously (Flajšman et al. 2016) and primers listed in Table 3. Before pathogenicity tests were carried out, fungal growth and conidiation were inspected as described previously (Flajšman et al. 2017b). Ten plants of the Verticillium wilt susceptible hop cultivar 'Celeia' were inoculated by 10-min root dipping in a conidia suspension (5×10^6 conidia/ml) of two arbitrarily selected *VnaChtBP* knockout mutants. Conidia of the wild type *V. nonalfalfae* isolate T2 served as a positive control and sterile distilled water was used as a mock control. Re-potted plants were grown under control conditions in a growth chamber (Flajšman et al. 2017b). Verticillium wilting symptoms were assessed five times over seven weeks post-inoculation using a disease severity index (DSI) with a 0-5 scale (Radišek et al. 2003). After symptom assessment, a fungal re-isolation test (Flajšman et al. 2017b) and qPCR using *V. nonalfalfae* specific primers (Cregeen et al. 2015) were performed to confirm infection of the tested hop plants.

Acknowledgments

This research was supported by the Slovenian Research Agency grants P4-0077, J4-8220 and fellowship 342257. This work benefitted from interactions promoted by the COST Action FA 1208 https://cost-sustain.org. The authors would like to thank Dr Vasja Progar for transcriptome analysis, Dr Vesna Hodnik for SPR analysis and Dr Miles Armstrong, Dr Marko Dolinar and Dr Jernej Jakše for technical advice.

Literature Cited

Abramyan, J., and Stajich, J. E. 2012. Species-specific chitin-binding module 18 expansion in the amphibian pathogen Batrachochytrium dendrobatidis. MBio. 3:e00150-12

Andersen, N. H., Cao, B., Rodríguez-Romero, A., and Arreguin, B. 1993. Hevein: NMR assignment and assessment of solution-state folding for the agglutinin-toxin motif. Biochemistry. 32:1407–22

Arnold, K., Bordoli, L., Kopp, J., and Schwede, T. 2006. The SWISS-MODEL workspace: a web-based environment for protein structure homology modelling. Bioinformatics. 22:195–201

Asensio, J. L., Cañada, F. J., Siebert, H.-C., Laynez, J., Poveda, A., Nieto, P. M., Soedjanaamadja, U., Gabius, H.-J., and Jiménez-Barbero, J. 2000. Structural basis for chitin recognition by defense proteins: GlcNAc residues are bound in a multivalent fashion by extended binding sites in hevein domains. Chem. Biol. 7:529–543

Böhm, H., Albert, I., Fan, L., Reinhard, A., and Nürnberger, T. 2014. Immune receptor complexes at the plant cell surface. Curr. Opin. Plant Biol. 20:47–54

Bohne, A., Lang, E., and von der Lieth, C.-W. 1998. W3-SWEET: Carbohydrate Modeling By Internet. J. Mol. Model. 4:33–43

Bohne, A., Lang, E., and von der Lieth, C. W. 1999. SWEET - WWW-based rapid 3D construction of oligo- and polysaccharides. Bioinformatics. 15:767–8

Boller, T., and Felix, G. 2009. A renaissance of elicitors: perception of microbe-associated molecular patterns and danger signals by pattern-recognition receptors. Annu. Rev. Plant Biol. 60:379–406

Bolton, M. D., van Esse, H. P., Vossen, J. H., de Jonge, R., Stergiopoulos, I., Stulemeijer, I. J. E., van den Berg, G. C. M., Borrás-Hidalgo, O., Dekker, H. L., de Koster, C. G., de Wit, P. J. G. M., Joosten, M. H. A. J., and Thomma, B. P. H. J. 2008. The novel Cladosporium fulvum lysin motif effector Ecp6 is a virulence factor with orthologues in other fungal species. Mol. Microbiol. 69:119–36

van den Burg, H. A., Harrison, S. J., Joosten, M. H. A. J., Vervoort, J., and de Wit, P. J. G. M. 2006. Cladosporium fulvum Avr4 protects fungal cell walls against hydrolysis by plant chitinases accumulating during infection. Mol. Plant. Microbe. Interact. 19:1420–30

van den Burg, H. A., Spronk, C. A. E. M., Boeren, S., Kennedy, M. A., Vissers, J. P. C., Vuister, G. W., de Wit, P. J. G. M., and Vervoort, J. 2004. Binding of the AVR4 elicitor of Cladosporium fulvum to chitotriose units is facilitated by positive allosteric protein-protein interactions: the chitin-binding site of AVR4 represents a novel binding site on the folding scaffold shared between the inverte. J. Biol. Chem. 279:16786–96

Cao, Y., Liang, Y., Tanaka, K., Nguyen, C. T., Jedrzejczak, R. P., Joachimiak, A., and Stacey, G. 2014. The

kinase LYK5 is a major chitin receptor in Arabidopsis and forms a chitin-induced complex with related kinase CERK1. Elife. 3

Cregeen, S., Radišek, S., Mandelc, S., Turk, B., Štajner, N., Jakše, J., and Javornik, B. 2015. Different Gene Expressions of Resistant and Susceptible Hop Cultivars in Response to Infection with a Highly Aggressive Strain of Verticillium albo-atrum. Plant Mol. Biol. Rep. 33:689–704

Dawson, N. L., Sillitoe, I., Lees, J. G., Lam, S. D., and Orengo, C. A. 2017. CATH-Gene3D: Generation of the resource and its use in obtaining structural and functional annotations for protein sequences. Pages 79–110 in: Methods in Molecular Biology,

Dodds, P. N., and Rathjen, J. P. 2010. Plant immunity: towards an integrated view of plant-pathogen interactions. Nat. Rev. Genet. 11:539–48

Dou, D., and Zhou, J.-M. 2012. Phytopathogen Effectors Subverting Host Immunity: Different Foes, Similar Battleground. Cell Host Microbe. 12:484–495

Duan, Y., Wu, C., Chowdhury, S., Lee, M. C., Xiong, G., Zhang, W., Yang, R., Cieplak, P., Luo, R., Lee, T., Caldwell, J., Wang, J., and Kollman, P. 2003. A point-charge force field for molecular mechanics simulations of proteins based on condensed-phase quantum mechanical calculations. J. Comput. Chem. 24:1999–2012

van Esse, H. P., Bolton, M. D., Stergiopoulos, I., de Wit, P. J. G. M., and Thomma, B. P. H. J. 2007. The chitin-binding Cladosporium fulvum effector protein Avr4 is a virulence factor. Mol. Plant. Microbe. Interact. 20:1092–101

Finn, R. D., Bateman, A., Clements, J., Coggill, P., Eberhardt, R. Y., Eddy, S. R., Heger, A., Hetherington, K., Holm, L., Mistry, J., Sonnhammer, E. L. L., Tate, J., and Punta, M. 2014. Pfam: The protein families database. Nucleic Acids Res. 42:222–230

Flajšman, M., Mandelc, S., Radišek, S., and Javornik, B. 2017a. Xylem sap extraction method from hop plants. Bio-Protocol. 7:1–11

Flajšman, M., Mandelc, S., Radišek, S., Štajner, N., Jakše, J., Košmelj, K., and Javornik, B. 2016. Identification of Novel Virulence-Associated Proteins Secreted to Xylem by Verticillium nonalfalfae During Colonization of Hop Plants. Mol. Plant-Microbe Interact. 29:362–373

Flajšman, M., Radišek, S., and Javornik, B. 2017b. Pathogenicity Assay of Verticillium nonalfalfae on Hop Plants. Bio-protocol. 7:e2171

Gubaeva, E., Gubaev, A., Melcher, R., Cord-Landwehr, S., Singh, R., El Gueddari, N. E., and Moerschbacher, B. M. 2018. 'Slipped sandwich' model for chitin and chitosan perception in Arabidopsis. Mol. Plant-Microbe Interact. :MPMI-04-18-0098-R

Guillén, D., Sánchez, S., and Rodríguez-Sanoja, R. 2010. Carbohydrate-binding domains: multiplicity of biological roles. Appl. Microbiol. Biotechnol. 85:1241–1249

Gust, A. A., Willmann, R., Desaki, Y., Grabherr, H. M., and Nürnberger, T. 2012. Plant LysM proteins: modules mediating symbiosis and immunity. Trends Plant Sci. 17:495–502

Hayafune, M., Berisio, R., Marchetti, R., Silipo, A., Kayama, M., Desaki, Y., Arima, S., Squeglia, F., Ruggiero, A., Tokuyasu, K., Molinaro, A., Kaku, H., and Shibuya, N. 2014. Chitin-induced activation of

563 immune signaling by the rice receptor CEBiP relies on a unique sandwich-type dimerization. Proc.
564 Natl. Acad. Sci. U. S. A. 111:E404-13

565 Hurlburt, N. K., Chen, L.-H., Stergiopoulos, I., and Fisher, A. J. 2018. Structure of the Cladosporium fulvum
566 Avr4 effector in complex with (GlcNAc)6 reveals the ligand-binding mechanism and uncouples its
567 intrinsic function from recognition by the Cf-4 resistance protein Y. Wang, ed. PLOS Pathog.
568 14:e1007263

569 Jakše, J., Čerenak, A., Radišek, S., Satovic, Z., Luthar, Z., and Javornik, B. 2013. Identification of
570 quantitative trait loci for resistance to Verticillium wilt and yield parameters in hop (Humulus
571 lupulus L.). Theor Appl Genet.

572 Jakše, J., Jelen, V., Radišek, S., de Jonge, R., Mandelc, S., Majer, A., Curk, T., Zupan, B., Thomma, B. P. H.
573 J., and Javornik, B. 2018. Genome sequence of xylem-invading Verticillium nonalfalfae lethal strain.
574 Genome Announc. 6:e01458-17

575 Jiménez-Barbero, J., Javier Cañada, F., Asensio, J. L., Aboitiz, N., Vidal, P., Canales, A., Groves, P., Gabius,
576 H.-J., and Siebert, H.-C. 2006. Hevein Domains: An Attractive Model to Study Carbohydrate–Protein
577 Interactions at Atomic Resolution. Adv. Carbohydr. Chem. Biochem. 60:303–354

578 Jones, J. D. G., and Dangl, J. L. 2006. The plant immune system. Nature. 444:323–9

579 de Jonge, R., Peter van Esse, H., Kombrink, A., Shinya, T., Desaki, Y., Bours, R., van der Krol, S., Shibuya,
580 N., Joosten, M. H. A. J., and Thomma, B. P. H. J. 2010. Conserved Fungal LysM Effector Ecp6
581 Prevents Chitin-Triggered Immunity in Plants. Science (80-.). 329:953–955

582 Kastritis, P. L., and Bonvin, A. M. J. J. 2013. On the binding affinity of macromolecular interactions: daring
583 to ask why proteins interact. J. R. Soc. Interface. 10:20120835

584 Kombrink, A., Rovenich, H., Shi-Kunne, X., Rojas-Padilla, E., van den Berg, G. C. M., Domazakis, E., de
585 Jonge, R., Valkenburg, D. J., Sánchez-Vallet, A., Seidl, M. F., and Thomma, B. P. H. J. 2017.
586 Verticillium dahliae LysM effectors differentially contribute to virulence on plant hosts. Mol. Plant
587 Pathol. 18:596–608

588 Krieger, E., and Vriend, G. 2015. New ways to boost molecular dynamics simulations. J. Comput. Chem.
589 36:996–1007

590 Krieger, E., and Vriend, G. 2014. YASARA View - molecular graphics for all devices - from smartphones to
591 workstations. Bioinformatics. 30:2981–2

592 Lerner, D. R., and Raikhel, N. V. 1992. The gene for stinging nettle lectin (Urtica dioica agglutinin)
593 encodes both a lectin and a chitinase. J. Biol. Chem. 267:11085–91

594 Li, W., Cowley, A., Uludag, M., Gur, T., McWilliam, H., Squizzato, S., Park, Y. M., Buso, N., and Lopez, R.
595 2015. The EMBL-EBI bioinformatics web and programmatic tools framework. Nucleic Acids Res.
596 43:W580-4

597 Liu, P., and Stajich, J. E. 2015. Characterization of the Carbohydrate Binding Module 18 gene family in the
598 amphibian pathogen Batrachochytrium dendrobatidis. Fungal Genet. Biol. 77:31–39

599 Liu, S., Wang, J., Han, Z., Gong, X., Zhang, H., and Chai, J. 2016. Molecular Mechanism for Fungal Cell Wall
600 Recognition by Rice Chitin Receptor OsCEBiP. Structure. 24:1192–1200

601 Liu, T., Liu, Z., Song, C., Hu, Y., Han, Z., She, J., Fan, F., Wang, J., Jin, C., Chang, J., Zhou, J.-M., and Chai, J.
602 2012. Chitin-induced dimerization activates a plant immune receptor. Science. 336:1160–4

603 Liu, W., Xie, Y., Ma, J., Luo, X., Nie, P., Zuo, Z., Lahrmann, U., Zhao, Q., Zheng, Y., Zhao, Y., Xue, Y., and
604 Ren, J. 2015. IBS: An illustrator for the presentation and visualization of biological sequences.
605 Bioinformatics. 31:3359–3361

606 Lombard, V., Golaconda Ramulu, H., Drula, E., Coutinho, P. M., and Henrissat, B. 2014. The carbohydrate-
607 active enzymes database (CAZy) in 2013. Nucleic Acids Res. 42:D490-5

608 Macho, A. P., and Zipfel, C. 2014. Plant PRRs and the activation of innate immune signaling. Mol. Cell.
609 54:263–72

610 Mandelc, S., and Javornik, B. 2015. The secretome of vascular wilt pathogen Verticillium albo-atrum in
611 simulated xylem fluid. Proteomics. 15:787–797

612 Marshall, R., Kombrink, A., Motteram, J., Loza-Reyes, E., Lucas, J., Hammond-Kosack, K. E., Thomma, B. P.
613 H. J., and Rudd, J. J. 2011. Analysis of two in planta expressed LysM effector homologs from the
614 fungus Mycosphaerella graminicola reveals novel functional properties and varying contributions to
615 virulence on wheat. Plant Physiol. 156:756–69

616 Marton, K., Flajšman, M., Radišek, S., Košmelj, K., Jakše, J., Javornik, B., and Berne, S. 2018.
617 Comprehensive analysis of Verticillium nonalfalfae in silico secretome uncovers putative effector
618 proteins expressed during hop invasion Z. Zhang, ed. PLoS One. 13:e0198971

619 Mentlak, T. a., Kombrink, A., Shinya, T., Ryder, L. S., Otomo, I., Saitoh, H., Terauchi, R., Nishizawa, Y.,
620 Shibuya, N., Thomma, B. P. H. J., and Talbot, N. J. 2012. Effector-Mediated Suppression of Chitin-
621 Triggered Immunity by Magnaporthe oryzae Is Necessary for Rice Blast Disease. Plant Cell. 24:322–
622 335

623 Miya, A., Albert, P., Shinya, T., Desaki, Y., Ichimura, K., Shirasu, K., Narusaka, Y., Kawakami, N., Kaku, H.,
624 and Shibuya, N. 2007. CERK1, a LysM receptor kinase, is essential for chitin elicitor signaling in
625 Arabidopsis. Proc. Natl. Acad. Sci. U. S. A. 104:19613–8

626 Mochizuki, S., Saitoh, K. ichiro, Minami, E., and Nishizawa, Y. 2011. Localization of probe-accessible chitin
627 and characterization of genes encoding chitin-binding domains during rice-Magnaporthe oryzae
628 interactions. J. Gen. Plant Pathol. 77:163–173

629 Möller, E. M. M., Bahnweg, G., Sandermann, H., and Geiger, H. H. H. 1992. A simple and efficient
630 protocol for isolation of high molecular weight DNA from filamentous fungi, fruit bodies, and
631 infected plant tissues. Nucleic Acids Res. 20:6115–6

632 Progar, V., Jakše, J., Štajner, N., Radišek, S., Javornik, B., and Berne, S. 2017. Comparative transcriptional
633 analysis of hop responses to infection with Verticillium nonalfalfae. Plant Cell Rep. 36:1599–1613

634 Qi, X., Sun, Y., and Xiong, S. 2015. A single freeze-thawing cycle for highly efficient solubilization of
635 inclusion body proteins and its refolding into bioactive form. Microb. Cell Fact. 14

636 R Core Team. 2016. R: A Language and Environment for Statistical Computing.

637 Radišek, S., Jakše, J., and Javornik, B. 2004. Development of pathotype-specific SCAR markers for
638 detection of Verticillium albo-atrum isolates from hop. Plant Dis. 88:1115–1122

639 Radišek, S., Jakše, J., and Javornik, B. 2006. Genetic variability and virulence among Verticillium albo-
640 atrum isolates from hop. Eur. J. plant Pathol. 116:301–314

641 Radišek, S., Jakše, J., Simončič, A., and Javornik, B. 2003. Characterization of Verticillium albo-atrum Field
642 Isolates Using Pathogenicity Data and AFLP Analysis. Plant Dis. 87:633–638

643 Ranf, S. 2017. Sensing of molecular patterns through cell surface immune receptors. Curr. Opin. Plant
644 Biol. 38:68–77

645 Sanchez-Vallet, A., Mesters, J. R., and Thomma, B. P. H. J. 2014. The battle for chitin recognition in plant-
646 microbe interactions. FEMS Microbiol. Rev. 39:171–83

647 Sánchez-Vallet, A., Saleem-Batcha, R., Kombrink, A., Hansen, G., Valkenburg, D.-J., Thomma, B. P. H. J.,
648 and Mesters, J. R. 2013. Fungal effector Ecp6 outcompetes host immune receptor for chitin binding
649 through intrachain LysM dimerization. Elife. 2:e00790

650 Schmittgen, T. D., and Livak, K. J. 2008. Analyzing real-time PCR data by the comparative C(T) method.
651 Nat. Protoc. 3:1101–8

652 Seidl, M. F., Faino, L., Shi-Kunne, X., van den Berg, G. C. M., Bolton, M. D., and Thomma, B. P. H. J. 2015.
653 The Genome of the Saprophytic Fungus *Verticillium tricorpus* Reveals a Complex Effector Repertoire
654 Resembling That of Its Pathogenic Relatives. Mol. Plant-Microbe Interact. 28:362–373

655 Shibuya, N., and Minami, E. 2001. Oligosaccharide signalling for defence responses in plant. Physiol. Mol.
656 Plant Pathol. 59:223–233

657 Shinya, T., Nakagawa, T., Kaku, H., and Shibuya, N. 2015. Chitin-mediated plant–fungal interactions:
658 catching, hiding and handshaking. Curr. Opin. Plant Biol. 26:64–71

659 Soanes, D. M., Alam, I., Cornell, M., Wong, H. M., Hedeler, C., Paton, N. W., Rattray, M., Hubbard, S. J.,
660 Oliver, S. G., and Talbot, N. J. 2008. Comparative genome analysis of filamentous fungi reveals gene
661 family expansions associated with fungal pathogenesis. PLoS One. 3:e2300

662 Sperschneider, J., Dodds, P. N., Singh, K. B., and Taylor, J. M. 2017. ApoplastP: prediction of effectors and
663 plant proteins in the apoplast using machine learning. doi.org. :182428

664 Spoel, S. H., and Dong, X. 2012. How do plants achieve immunity? Defence without specialized immune
665 cells. Nat. Rev. Immunol. 12:89–100

666 Stergiopoulos, I., van den Burg, H. A., Okmen, B., Beenen, H. G., van Liere, S., Kema, G. H. J., and de Wit,
667 P. J. G. M. 2010. Tomato Cf resistance proteins mediate recognition of cognate homologous
668 effectors from fungi pathogenic on dicots and monocots. Proc. Natl. Acad. Sci. 107:7610–5

669 Stergiopoulos, I., De Kock, M. J. D., Lindhout, P., and De Wit, P. J. G. M. 2007. Allelic variation in the
670 effector genes of the tomato pathogen Cladosporium fulvum reveals different modes of adaptive
671 evolution. Mol. Plant. Microbe. Interact. 20:1271–1283

672 Takahara, H., Hacquard, S., Kombrink, A., Hughes, H. B., Halder, V., Robin, G. P., Hiruma, K., Neumann, U.,
673 Shinya, T., Kombrink, E., Shibuya, N., Thomma, B. P. H. J., and O'Connell, R. J. 2016. Colletotrichum
674 higginsianum extracellular LysM proteins play dual roles in appressorial function and suppression of
675 chitin-triggered plant immunity. New Phytol. 211:1323–1337

676 Trott, O., and Olson, A. J. 2009. AutoDock Vina: Improving the speed and accuracy of docking with a new
677 scoring function, efficient optimization, and multithreading. J. Comput. Chem. 31:NA-NA

678 Waterhouse, A., Bertoni, M., Bienert, S., Studer, G., Tauriello, G., Gumienny, R., Heer, F. T., de Beer, T. A.
679 P., Rempfer, C., Bordoli, L., Lepore, R., and Schwede, T. 2018. SWISS-MODEL: homology modelling
680 of protein structures and complexes. Nucleic Acids Res. 46:W296–W303

681 Wright, H. T., Sandrasegaram, G., and Wright, C. S. 1991. Evolution of a family of N-acetylglucosamine
682 binding proteins containing the disulfide-rich domain of wheat germ agglutinin. J. Mol. Evol.
683 33:283–94

684

685

Tables

Table 1. The results of homology modelling of the VnaChtBP using the SWISS-MODEL server.

	Template	Description	Seq Identity	Oligo-States	GMOE	QMEAN	Coverage
Model01	2uwg.1.A	Wheat germ lectin	43.98%	Homo-dimer	0.31	-4.61	98-318
Model02	2wgc.1.A	Agglutin isolectin 1	40.96%	Homo-dimer	0.32	-3.22	39-254
Model03	1ulk.1.A	Lectin-C	49.15%	Homo-dimer	0.20	-0.65	212-378

Table 2. Comparison of chitin oligomer binding affinities of various fungal effectors and plant defense proteins, obtained using ITC or SPR.

Organism	**Protein**	**CAZy**	**Ligand**	**K_d (µM)**	**Method**	**Reference**
Verticillium nonalfalfae	VnaChtBP	CBM18	$(GlcNAc)_6$	0.78 ± 0.58	SPR	This study
Cladosporium fulvum	Avr4	CBM14	$(GlcNAc)_6$	6.3 ± 0.23	ITC	(van den Burg et al. 2004)
Cladosporium fulvum	Ecp6	CBM50	$(GlcNAc)_{4,5,6,8}$	11.5 to 3.7	ITC	(de Jonge et al. 2010)
Cladosporium fulvum	Ecp6	CBM50	$(GlcNAc)_8$	1.3×10^{-3}	SPR	(Mentlak et al. 2012)
Magnaporthe oryzae	Slp1	CBM50	$(GlcNAc)_8$	2.4×10^{-3}	SPR	(Mentlak et al. 2012)
Colletotrichum higginsianum	ChELP1	CBM50	$(GlcNAc)_8$-Bio	2.6×10^{-5}	SPR	(Takahara et al. 2016)
Colletotrichum higginsianum	ChELP2	CBM50	$(GlcNAc)_8$-Bio	2.5×10^{-4}	SPR	(Takahara et al. 2016)
Arabidopsis thaliana	AtLYK5	CBM50	$(GlcNAc)_8$	1.72	ITC	(Cao et al. 2014)
Arabidopsis thaliana	AtCERK1	CBM50	$(GlcNAc)_8$	455	ITC	(Cao et al. 2014)
Arabidopsis thaliana	AtCERK1	CBM50	$(GlcNAc)_8$	448	ITC	(Liu et al. 2012)
Hevea brasiliensis	Hevein	CBM18	$(GlcNAc)_5$	2.1	ITC	(Asensio et al. 2000)

ITC, isothermal titration calorimetry; SPR, surface plasmon resonance, CBM, carbohydrate-binding module; GlcNAc, N-Acetylglucosamin, Bio, biotinylated

Table 3. List of primers used for cloning, gene disruption and expression of *VnaChtBP*, and fungal identification.

PRIMER	SEQ 5' – 3'	NOTE
CBP_F	ATGCGTTTCTCCGCCGTTCTTA	Cloning of *VnaChtBP*
CBP_R	TTAGGTGCAGATACCAAAGGCACGCT	Cloning of *VnaChtBP*
Vna8.213-F	GCCAAGCCCCCCAAGA	*VnaChtBP 3* gene expression with RT-qPCR
Vna8.213-R	AAGAGGCGTCGTCGGAAAA	*VnaChtBP* gene expression with RT-qPCR
T7p	TAATACGACTCACTATAGGG	Vector primer for DNA sequencing
SP6	ATTTAGGTGACACTATAG	Vector primer for DNA sequencing
CBD_O1for	GGTCTTAAUTGGAACTTCTTTCGCAATCC	Preparation of *VnaChtBP* KO mutants
CBD_O2rev	GGCATTAAUGAGTGTGTCGACTAGGCTTGG	Preparation of *VnaChtBP* KO mutants
CBD_A3for	GGACTTAAUCGGCTGTGTTACATCACGTT	Preparation of *VnaChtBP* KO mutants
CBD_A4rev	GGGTTTAAUGTCGTTCTTCACCTCGCAAT	Preparation of *VnaChtBP* KO mutants
9-1gs-F	GGTAACGTCATCGAACGACATC	*V. nonalfalfae* detection (Radišek et al. 2004)
9-1gs-R	CACACGCTACATATCAAACAGCATAT	*V. nonalfalfae* detection (Radišek et al. 2004)

Figure captions

Fig. 1. Domain architecture (A-D) and gene expression (E) of CBM18-containing proteins identified in *Verticillium nonalfalfae*. Protein organization was determined by querying protein sequences against CATH-Gene3D (Dawson et al. 2017) using the FunFHMMer web server and presented by IBS software (Liu et al. 2015). Proteins were classified into four groups: Lectin-like proteins (A), Chitinases (B), Chitin deacetlyases (C) and Xyloglucan endotransglucosylase (D). Gene expression is presented as a heatmap of log_2CPM values determined by RNA sequencing of infected hop (Progar et al. 2017).

Fig. 2. *VnaChtBP*, a gene encoding the CBM18 chitin binding protein of *Verticillium nonalfalfae*, is highly expressed in stems of susceptible hop at the late stages of infection. The gene expression of *VnaChtBP* was quantified by RT-qPCR using a cDNA prepared from the roots and shoots of infected susceptible ('Celeia') and resistant ('Wye Target') hop plants (n = 5) at 6, 12 and 18 dpi and the expression levels were normalised relative to the expression of the gene in ½ liquid Czapek-Dox medium using topoisomerase (*VnaUn.148*) and splicing factor 3a2 (*Vna8.801*) as housekeeping genes (Marton et al. 2018). FC, fold change; dpi, days post inoculation.

Fig. 3. Confirmation of VnaChtBP dimerization (A) and schematic representation of the VnaChtBP homology model in complex with chitin hexamer (B). A: The effector gene *VnaChtBP* was cloned into the vectors pDEST22 and pDEST32 to serve both as bait and as prey and yeast-two-hybrid assay was performed. Weak dimerization of the effector was confirmed on a triple dropout reporter media SC-LWH and no self-activation of the pDEST22 construct with empty pDEST32 vector was detected on the X-gal reporter. B: The 3D model of VnaChtBP obtained by Swiss-Model (Arnold et al. 2006; Waterhouse et al. 2018) was refined by YASARA Structure (Krieger and Vriend 2014, 2015) and used in YASARA's AutoDock VINA module (Trott and Olson 2009) for molecular docking of chitin hexamer, built in the SWEET PROGRAM (Bohne et al. 1998, 1999). VnaChtBP is in dimeric form, the chitin binding domains of the Chain A (Chain B) are in cyan (grey) color shades. The chitin hexamer is shown in stick representation.

Fig. 4. A carbohydrate sedimentation test confirmed that the recombinant protein VnaChtBP specifically binds to chitin. A recombinant protein (15 µg) that bound to chitin beads and crab shell chitin was detected in the sediment, while it was present in the supernatant when incubated with cellulose, xylan or without the addition of carbohydrates (control). Western blot analysis was performed with primary antibody His-probe (H-3) (SCBT) (1:1,000) and secondary Chicken anti-mouse IgG-HRP (SCBT) (1:5,000). Protein bands were detected using Super Signal West Pico (ThermoFisher Scientific) ECL substrate in a GelDoc-It2 Imager (UVP).

Fig. 5. SPR analysis of chitin hexamer binding to VnaChtBP. Different concentrations (0.05, 0.1, 0.2, 0.4, 0.8, 1.6, 3.2 and 6.4 µM) of $(GlcNAc)_6$ were tested for the binding (top panel). The binding curve (bottom panel) was generated by fitting steady state response levels at the end of the association phase, versus the concentration of the injected chitin hexamer. K_d was obtained by fitting the data to the steady-state affinity model. For reproducibility of binding, three independent titration experiments were performed. $(GlcNAc)_6$, hexa-N-acetyl chitohexaose

732 **Fig 6.** VnaChtBP protects fungus against degradation by plant chitinases. Micrographs of *Trihoderma*
733 *viride* germinating spores, preincubated at RT for 2 h with 3 µM VnaChtBP, followed by the addition of
734 xylem sap (19 U of chitinase/mg total protein) from *V. nonalfalfae* infected hop, were taken 24 h after
735 treatment. The recombinant protein VnaChtBP caused aggregation and compaction of *T. viride* hyphae
736 and protected the fungus from degradation by xylem sap chitinases. The chitinase activity of xylem sap
737 was measured as a release of dye from Chitin Azure and one chitinase unit was defined as the amount of
738 enzyme that caused a 0.01 increase in absorbance at 575 nm, measured at pH 5.0 and 25°C.

739 **Fig. 7.** Symptom development in susceptible hop following infection with the wild type *V. nonalfalfae*
740 and two knockout mutants of *VnaChtBP*. Plants of susceptible hop 'Celeia' were inoculated by root
741 dipping in 5×10^6 conidia/ml suspension and Verticillium wilting symptoms were assessed five times post
742 inoculation. A: Both *VnaChtBP* deletion mutants displayed Verticillium wilting symptoms (chlorosis and
743 necrosis of the leaves) in susceptible hop similar to the wild type fungus. Pictures were taken 35 days
744 post inoculation. B: According to disease severity index (DSI) assessment with a 0-5 scale (Radišek et al.
745 2003) there were no significant differences between the wild type *V. nonalfalfae* and knockout mutants
746 of *VnaChtBP*. Means with SE were calculated for 10 plants per treatment. Dpi, days post inoculation.

747

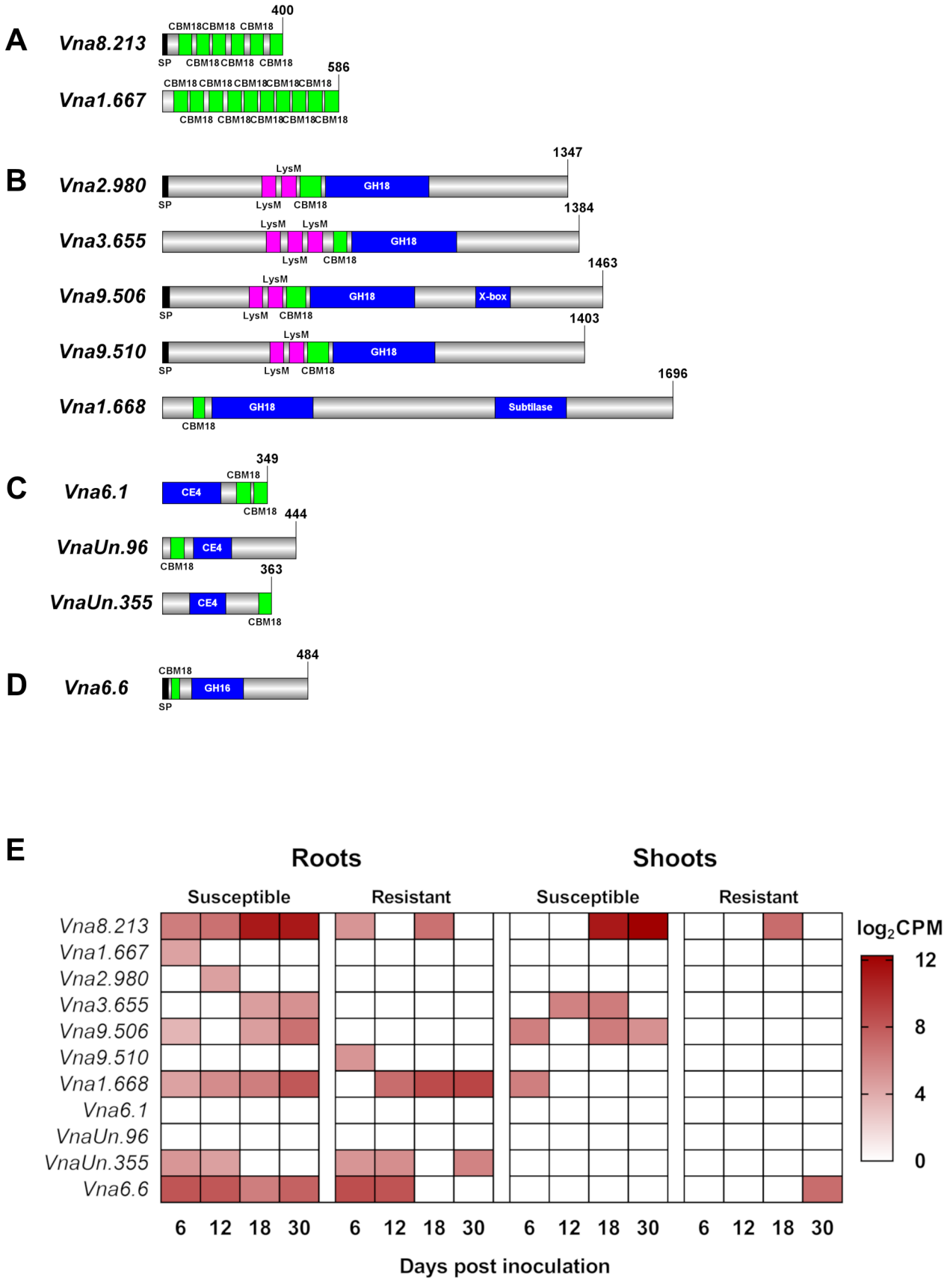
A
Vna8.213
400
CBM18 CBM18 CBM18
SP CBM18 CBM18 CBM18
Vna1.667
586
CBM18 CBM18 CBM18 CBM18 CBM18
CBM18 CBM18 CBM18 CBM18 CBM18
B
Vna2.980
1347
LysM
GH18
SP LysM CBM18
Vna3.655
1384
LysM LysM
GH18
LysM CBM18
Vna9.506
1463
LysM
GH18
X-box
SP LysM CBM18
Vna9.510
1403
LysM
GH18
SP LysM CBM18
Vna1.668
1696
GH18
Subtilase
CBM18
C
Vna6.1
349
CBM18
CE4
CBM18
VnaUn.96
444
CE4
CBM18
VnaUn.355
363
CE4
CBM18
D
Vna6.6
484
CBM18
GH16
SP
E
Roots
Shoots
Susceptible
Resistant
Susceptible
Resistant
Vna8.213
Vna1.667
Vna2.980
Vna3.655
Vna9.506
Vna9.510
Vna1.668
Vna6.1
VnaUn.96
VnaUn.355
Vna6.6
log2CPM
12
8
4
0
6 12 18 30 6 12 18 30 6 12 18 30 6 12 18 30
Days post inoculation

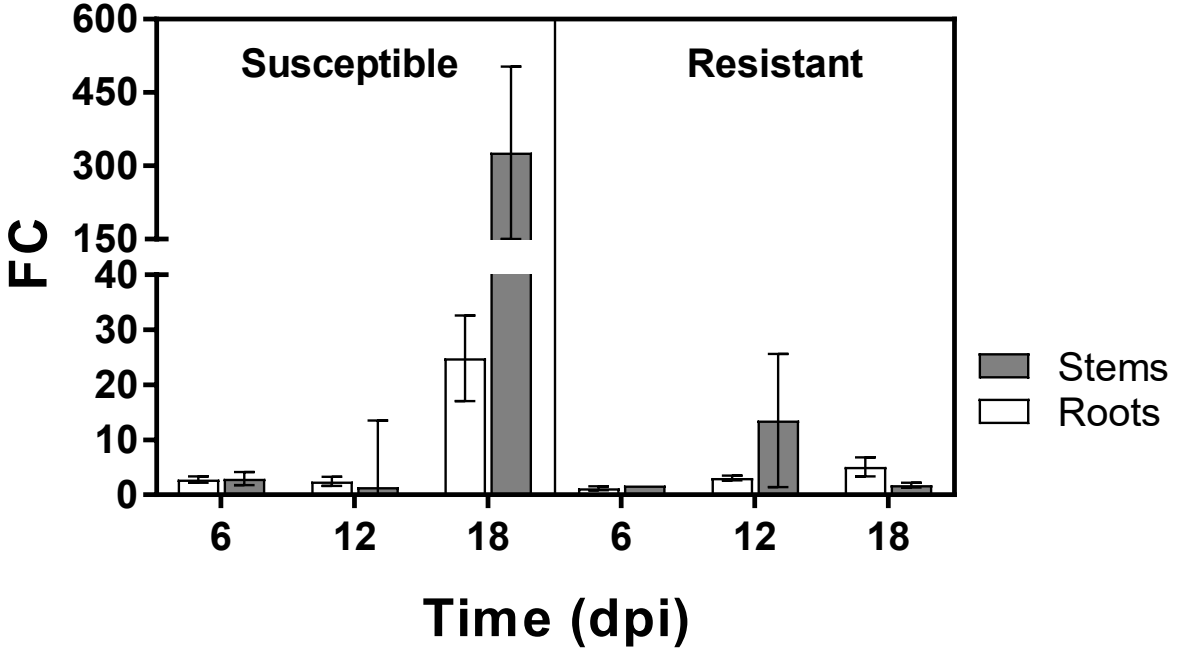
600
450
300
150
40
30
20
10
0
FC
Susceptible
Resistant
Stems
Roots
6
12
18
6
12
18
Time (dpi)

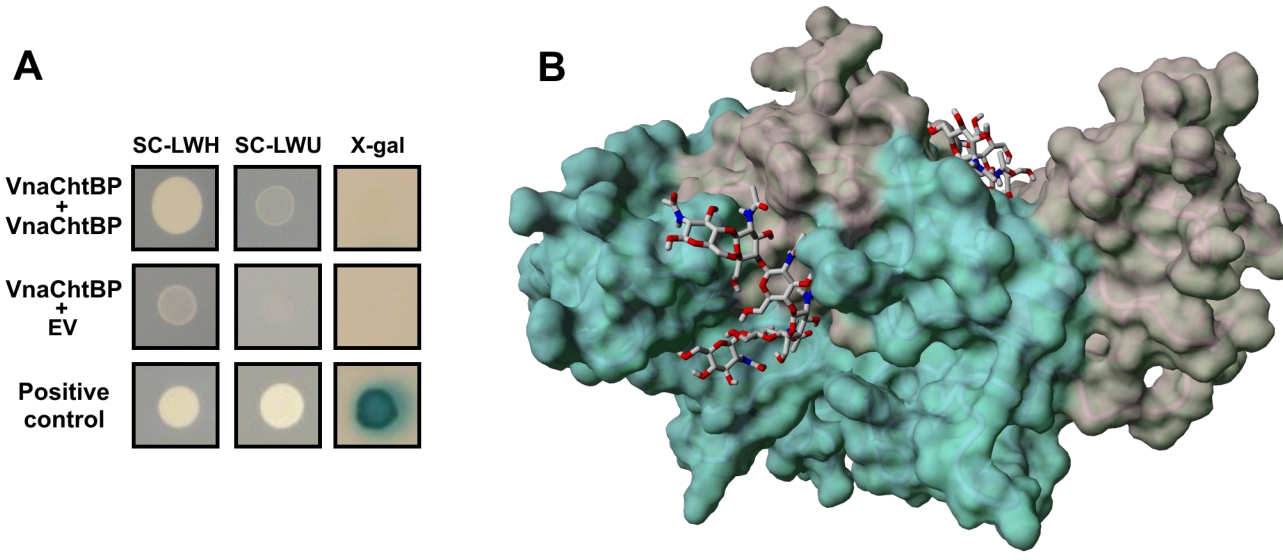
A
SC-LWH
SC-LWU
X-gal
VnaChtBP + VnaChtBP
VnaChtBP + EV
Positive control
B

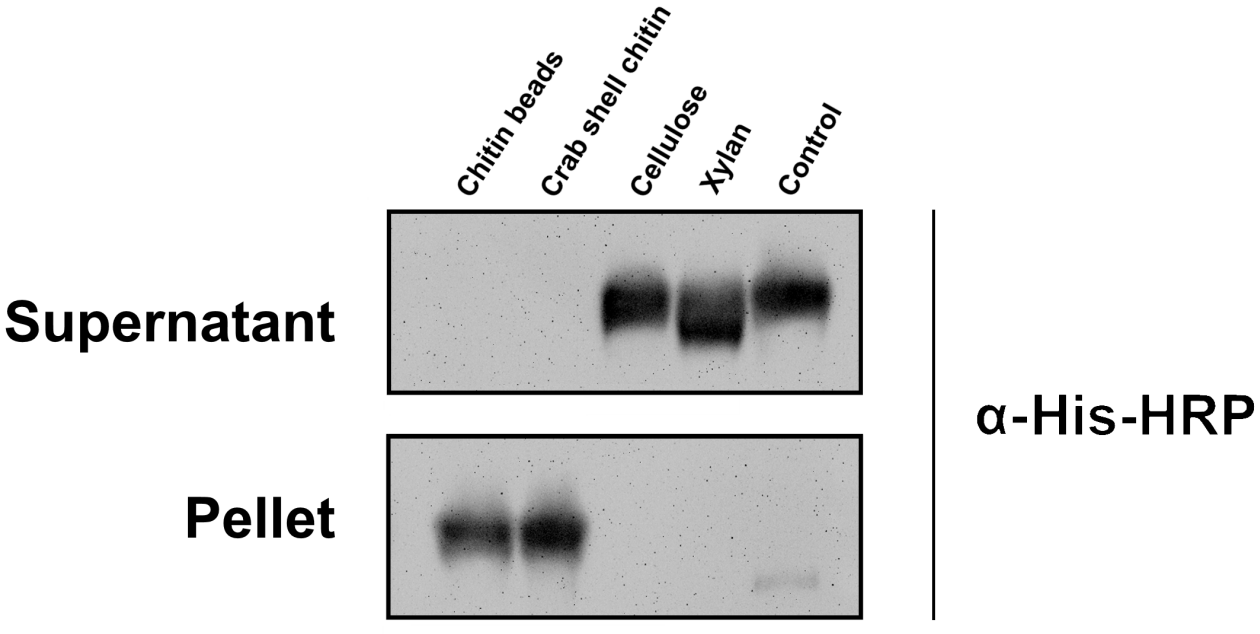
Chitin beads
Crab shell chitin
Cellulose
Xylan
Control
Supernatant
Pellet
α-His-HRP

A

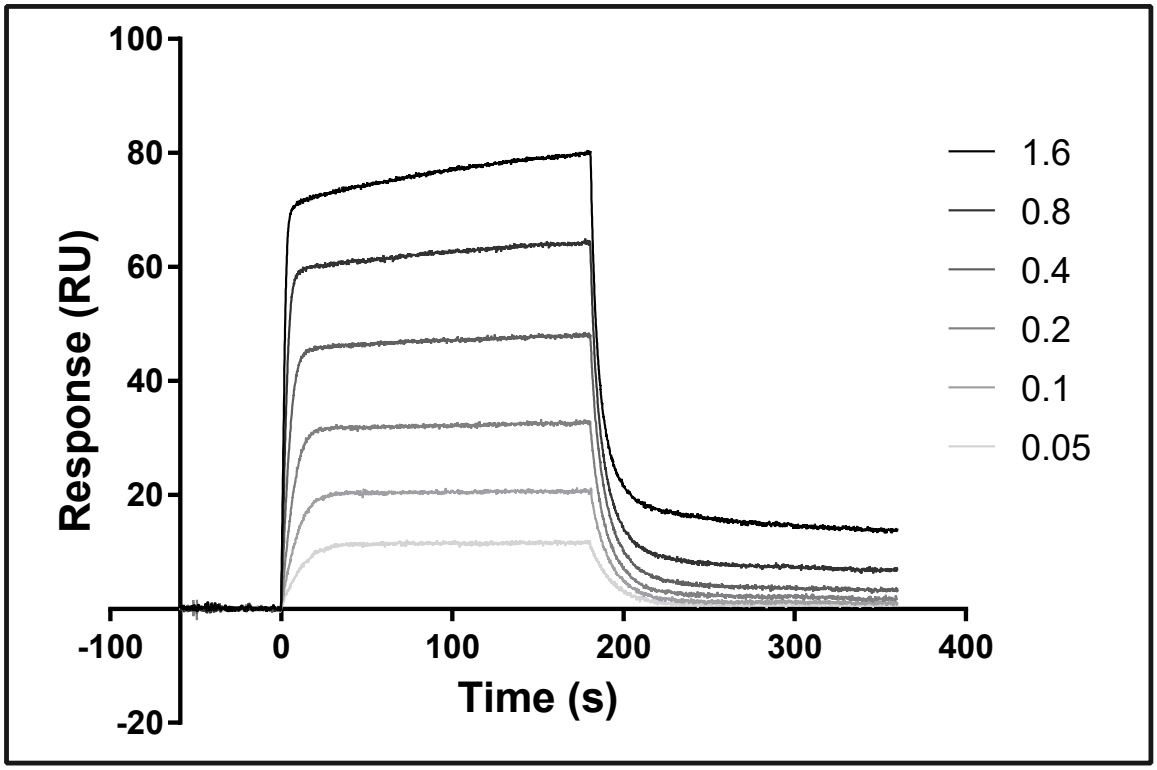
100
80
60
40
20
-20
Response (RU)
-100
0
100
200
300
400
Time (s)
1.6
0.8
0.4
0.2
0.1
0.05

B

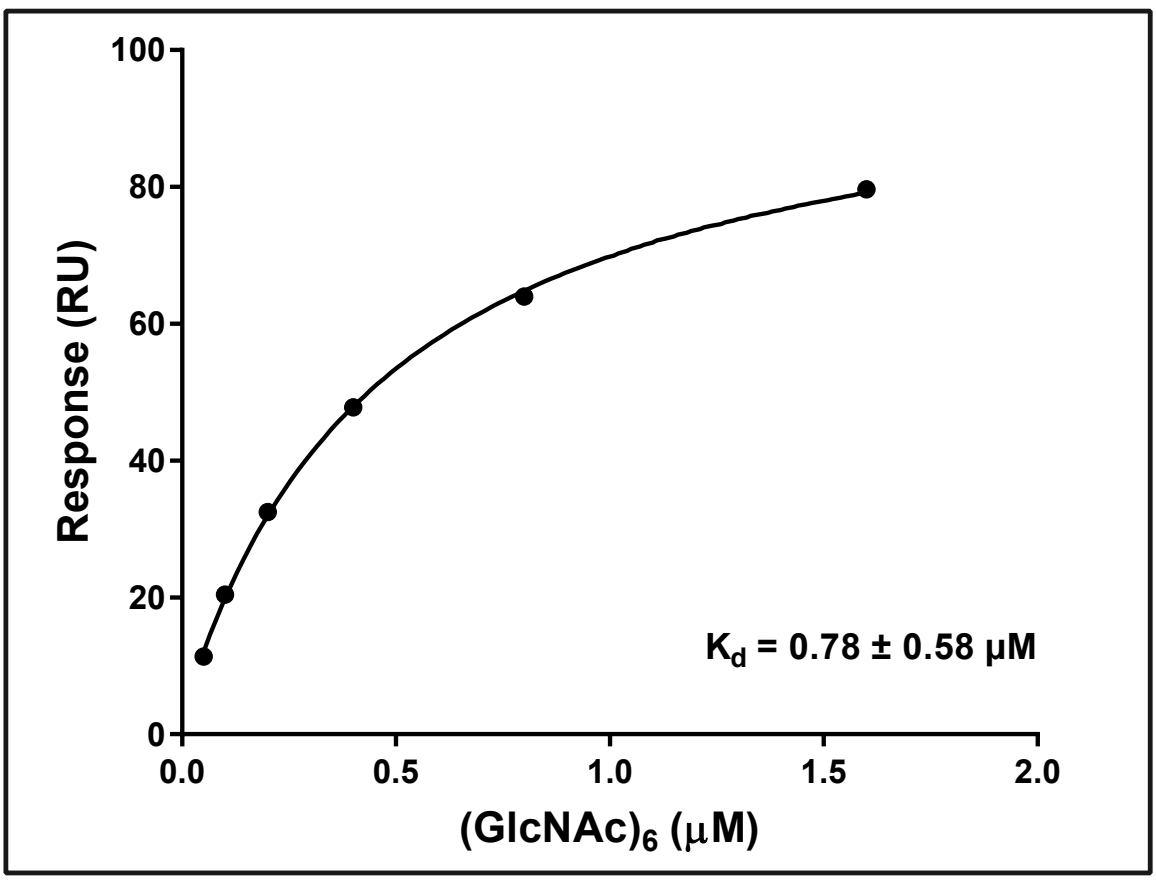
100
80
60
40
20
0
Response (RU)
0.0
0.5
1.0
1.5
2.0
(GlcNAc)6 (μM)
Kd = 0.78 ± 0.58 μM

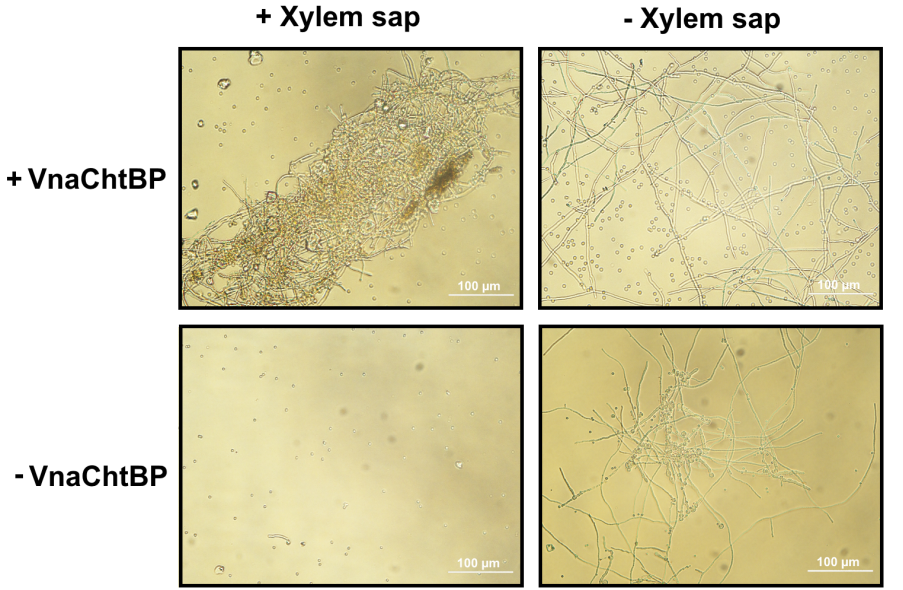
+ Xylem sap
- Xylem sap
+ VnaChtBP
- VnaChtBP
100 µm
100 µm
100 µm
100 µm

A

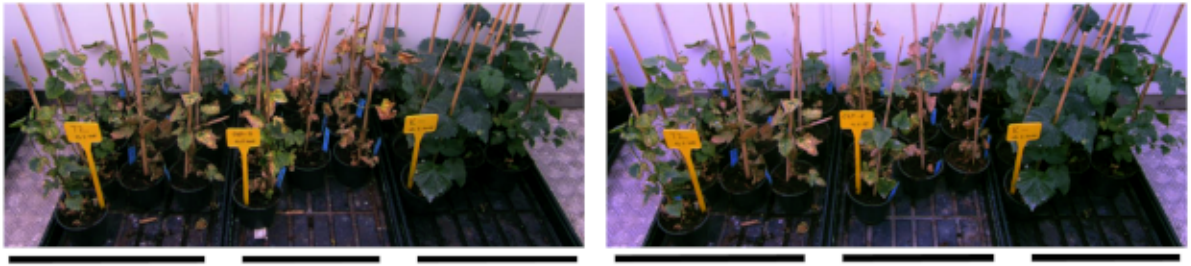
WT
ΔVnaChtBP-a
mock
WT
ΔVnaChtBP-b
mock

B

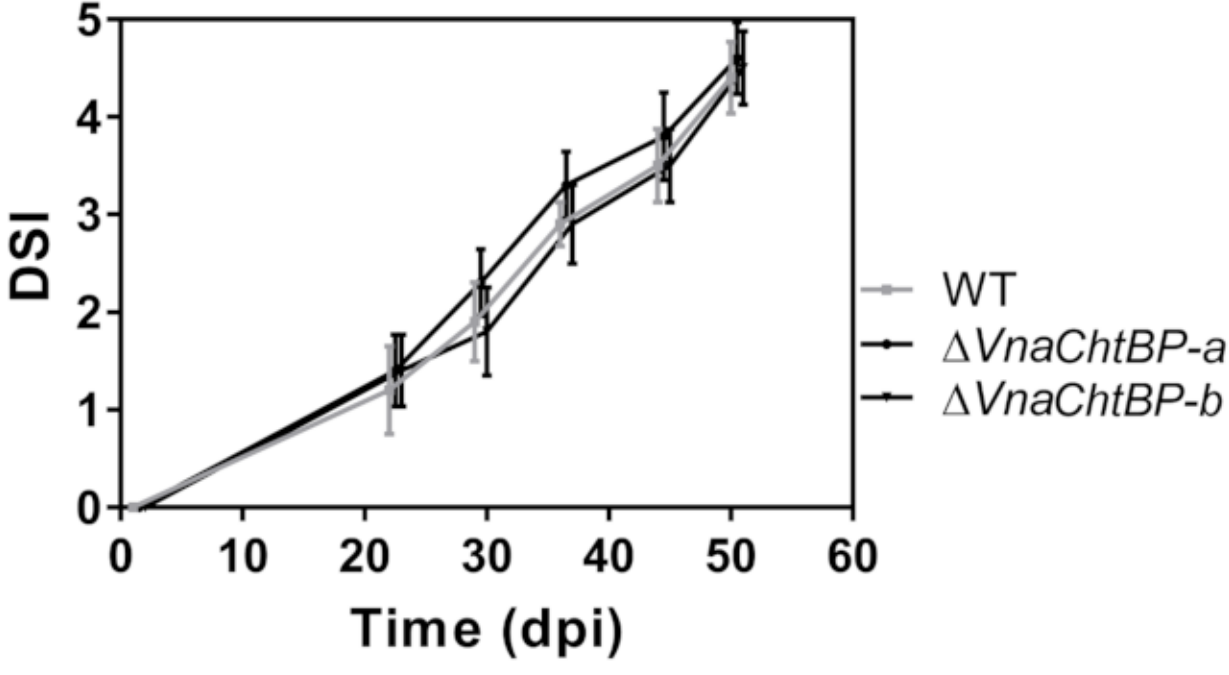
DSI
0
1
2
3
4
5
0
10
20
30
40
50
60
Time (dpi)
WT
ΔVnaChtBP-a
ΔVnaChtBP-b